FUDMA Journal of Sciences (FJS)
ISSN online: 2616-1370
ISSN print: 2645 - 2944
Vol. 9 No. 7, July, 2025, pp 262 – 267
DOI: https://doi.org/10.33003/fjs-2025-0907-3788

TOWARDS SUSTAINABLE SOLAR ENERGY STORAGE: A PATENT ANALYSIS FOR IMPROVING ENERGY DENSITY, CYCLE DURABILITY AND RATE CAPACITY FOR HYBRID LITHIUM-ION BATTERY (LiFePO$_4$)

***Adamu S. Gene, Yakubu Adamu and Baba Alfa**

Department of Physics, Faculty of Applied Science, Ibrahim Badamasi Babangida University Lapai, Nigeria

*Corresponding authors' email: genesalahudeen@gmail.com

ABSTRACT

The adoption of renewable energy is accelerating globally in wind and solar energy generation, solar energy particularly provides the promising outlook, its availability and flexibility of use makes it the most acceptable energy source required to achieve high perceptions of intermittent renewable energy. Despite this, solar energy storage capacity is currently underutilized in terms of minutes to hours of output at full power capacity. Although, research efforts and resource planning have begun to forecast on large-scale solar energy storage for a long duration, none has achieved a larger power capacity for a long duration. To this end, we explored the essentials of long-duration energy storage systems by analysing energy density, cycle durability and capacity rating for Hybrid Lithium-ion Battery (LiFePO4). In doing so, major components of potential long-duration storage values and their sensitivity to key parameters were assessed and the resulting indicators compared. The study showed a fast response time with improved energy density leading to a relatively high efficiency of about 42% as compare to the standard roundtrip efficiency of 45%. Cycle durability was highly influenced by depth of discharge (DoD), leading to a relatively short 3.5-hour lifetime for charge management, which is common when considering typical battery behaviour. Thus, strategies identified to improve Li-ion batteries: finding alternative electrode materials to improve energy density, decrease the environmental and societal impact of the raw materials, implementing self-healing mechanisms to improve cycle lifetime, and improving the efficiency to decrease costs.

Keywords: Energy Density, Cycle durability, Rate capacity, Lithium-ion Battery (LiFePO4)

INTRODUCTION

The current drive to progress renewable energy technology in light of the global energy demand for the expansion of the economy has become more challenging than ever. There is the growing demand for energy both at industrial and household sector, yet there are mainly dependent on the grid system. Thus, considering the unsustainable nature of nonrenewable energy resources and their impact on climate change, the combination of renewable energy sources with high standard energy storage option carries great promise for a cleaner, more efficient energy future, particularly for the housing and buildings sector in countryside (Sayed *et. al.,* 2023). Solar cells and metal-based batteries are a few examples of clean and sustainable energy technologies that are so pervasive. However, the unpredictable availability of renewable electricity sources necessitates the rapid development of energy storage technologies that are sustainable. These requirements are the outcome of an effort to advance an eco-friendly solar energy storage that favors the use of clean energy, rather than continually depleting nonrenewable natural resources, in order to support a healthy environment **(**Holechek *et al.,* 2022**).**

This has led to tremendous recent advances in energy storage in terms of adaptability, high energy density, cycle durability, rate capacity and efficiency (Divya *et al.,* 2009). More self-sustaining approaches to energy management are being looked into as a result of the world's rapidly expanding population, which will result in a higher rate of resource use (Wang *et al.,* 2021). The metal-ion battery is one of the most important inventions for assisting with energy supply and management (Abakumov *et al.,* 2020). LIBs have been explored as one of the most developed power supply technologies with high charge–discharge current (Nazri *et al.,* 2003).

LIBs are known to be lightweight, more compact, design flexible, able to operate at a voltage of 3.6 to 4 V, and have a capacity ranging from 700 to 2400 mAh for a single cell battery (Reddy *et al.,* 2013, BU-302, 2023). Although lithium metal batteries theoretically have far higher energy densities than LIBs, overuse and vulnerability will cause an explosion because of their low recharge ability (Deng, 2015). The development of materials for use in LIB devices has also been the subject of extensive research during the past several years (Atawi *et al.,* 2022). The nanoscale ranges in engineering electrode materials are known to be important in the field of electrochemical energy storage (Wang *et al.,* 2016). Presently, a variety of nanostructures, including zero-, one-, two-, and three dimensional ones, have been developed using complementary electrode materials. Despite this, a significant amount of improvement on LIB storage capacity is required in order to meet up with the daily power demand for solar storage. Thus, improvement on energy density, cycle durability, rate capacity and nanostructured material can widen the scope and challenges based on improving energy storage. The present work focuses on the development and analysis for improving energy density, cycle durability and rate capacity for the next-generation hybrid lithium-ion battery (LiFePO$_4$). To this end, we anticipate that this analysis will not only give a thorough overview of recent developments in improving storage capacity but will also throw light on the potential future development of unique battery technologies that is sustainable and eco-friendly.

MATERIALS AND METHODS

Lithium-ion Battery (LiFePO$_4$).

The Lithium Batteries (LiFePO$_4$) are commonly use nowadays for solar energy storage, this is due to their effectiveness in storing energy, ease of upkeep, extended lifespan, stability and temperature tolerance, this allow them to be used for higher-level applications (Islam *et al.,* 2010). In addition, the iron (Fe) transition metal is inexpensive, accessible, and environmentally sustainable (Wu *et al.,* 2018).

Regardless of the beneficial factors, LiFePO4 is a poor conductor of electricity and the charging voltage is between 3.5V- 4V for each cell (Shukla *et al.,* 2008). In spite of this, two methods were implemented in order to improve it storage capacity. The first technique involves reducing the particles size to enhance the energy density and the second involves using the conductive carbon nanostructure of LiFePO4 (Shukla *et al.,* 2008).

For charging process, the electrical supply is connected to two electrodes, the electron is then driven to leave the cathode to the anode, and while moving from cathode to anode through the electrolyte, the lithium do so concurrently in the same direction. The reactions which occur through the lithium-ion and electron generation are as follows

At the Anode

$$6C + xLi^{+} + xe^{-} \leftrightarrow Li_{x}C_{6} \qquad (1)$$

At the cathode

$$\mathrm{Li}C_{O}O_{2} \leftrightarrow +Li_{x}C_{O}O_{2} + Li^{+} + xe^{-} \qquad (2)$$

To transit energy during the discharge process, the electron from the anode travel to the cathode through the wire that passes through an external load. This occurs simultaneously from both anode to cathode as shown in figure 1.

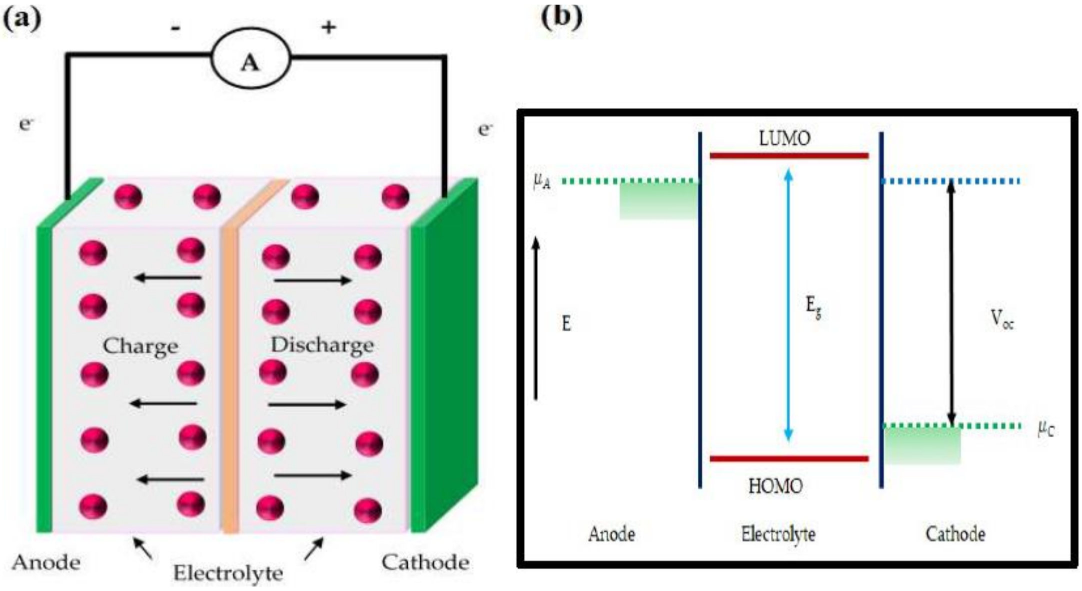

Figure 1: (a) Schematic diagram of a lithium-ion battery and (b) electrode potentials and the electrolyte energy gaps relative energies in LIBs (Zhang *et al.,* 2018, John, 2011)

Battery packs are used in the assemblage of the battery cell. The process involves numerous battery cells merging to form a module which results in a battery pack (Deng, 2015). Furthermore, optimal efforts can be acquired based on the electrode materials, especially for the anode and cathode (Liu *et al.,* 2016). This depends upon their electrochemical potential values; in which mA is known as the anode and mC is known as the cathode (Roy and Srivastava, 2015). To achieve a stable cell, mA is required to have a lower energy compared to the LUMO of the electrolyte. Thus, the electrolyte will be reduced, thereby having a greater energy than the HOMO of the electrolyte (John, 2011). Moreover, high lithium intercalation power and the greatest electrochemical potential difference between the anode and the cathode may be used to achieve high energy storage density (Liu and Cao, 2010). A variety of factors, including specific energy, volumetric energy, particular capacity, abuse tolerance, and discharging rate, affect how effectively LIBs function.

Research Design Methodology

Improving Energy Density

Today's lithium ion batteries have an energy density of 200-300 Wh/kg (Kowitkulkrai *et al.,* 2019). In other words, there is 4kg of material per kWh of energy storage, of this material build-up, 2 kg is in the cathode, 1 kg is in the anode, 0.6 kg in the current collectors, 0.3 kg in the electrolyte and 0.1 kg in the balance. In this research work, we introduces $Li[Ni_{0.92}Co_{0.06}Al_{0.01}Nb_{0.01}]O_2$ (Nb-NCA93) cathode with a high energy of 869 Wh kg^{-1}. The presence of Nb in the Nb-NCA93 cathode induces the grain refinement of its secondary particle thus, alleviating internal stress and preventing heteroneity of Li concentration during cycling. Therefore, the resulting full-cell reaches full charge within 12-15 minute and retains 85.3% of its initial capacity rating after 1000 cycles (cycle at full depth of discharge). In addition, the Nb-NCA93 cathode generates limited heat under XFC conditions due to refined nanostructure. The high lithium intercalation power produced after the introduction of $Li[Ni_{0.92}Co_{0.06}Al_{0.01}Nb_{0.01}]O_2$ (Nb-NCA93) which generate a high electrochemical potential difference between the anode and the cathode was used to achieve high energy storage density in this research work.

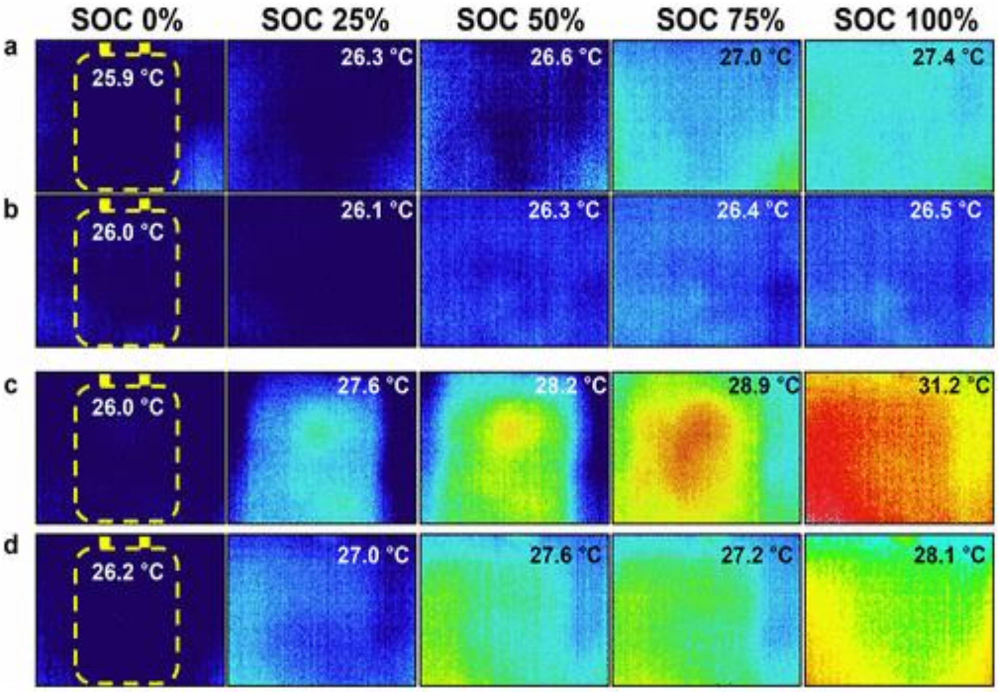

Figure 2: Thermal images of (a) NCA93- and (b) Nb-NCA93-based cells charged at 0.1 C and (c) NCA93- and (d) Nb-NCA93-based cells charged at 3 C. [23]

RESULTS AND DISCUSSION

Lifecycle Durability and Sensitivity to Temperature

The lifecycle durability and temperature distribution characteristics of the LiB for this works were investigated using thermogams at a maximum temperature point of 3C-rate. A comparison of cells between the LiB (A-1) and a supplier Type SUPPER B (B-1) was conducted. The result shows that A-1 cell has higher sensitivity to temperature change than the edge and it is observed that the temperature of the surface near left tab is relatively low. Meanwhile, the entire active area of the B-2 cell is hotter than the rest, and the left part is observed to be hotter than the right. Histogram was utilized for numerical analysis of the temperature distribution as shown in figure 3. The average temperature of the active area of B-2 is 14.6 °C higher than A-1. In temperature standard deviation (σ) comparison of the active areas between A-1 and B-2, A-1 had a denser temperature distribution than B-2, an indication that the lower temperature distribution of the top part of the cell contributes to a longer lifecycle. In summary, A-1 cell showed better results than B- 2 in terms of operating temperature, lifecycle durability and distribution characteristics.

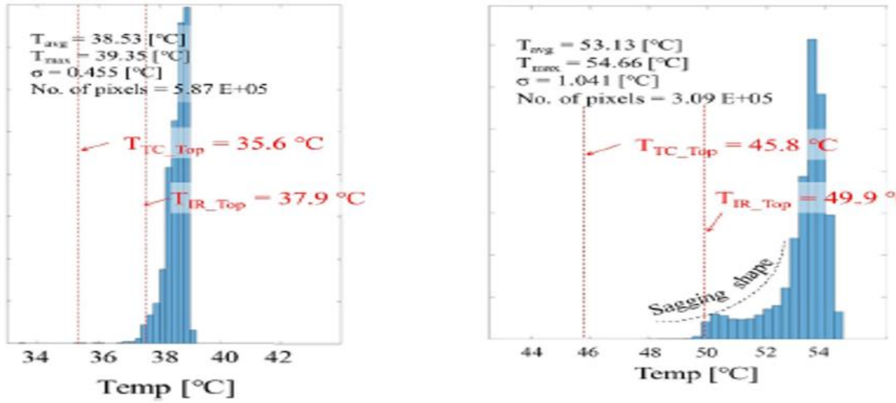

Figure 3: Temperature distribution of A-1 and B-2

Figure 4 shows the sensitivity test to temperature of cycling aging A-1 series cells. It is observed that the lifespan decreased by about 17.0% when the ambient temperature increased by 4 °C. A-series battery experiences a negative 4.25% / °C lifespan change when the ambient temperature increases near room temperature. Fig.4 (b) shows the normalized sensitivity to the temperature of A-1 and B-1 batteries from 15 to 40 °C. It is confirmed that the sensitivity of A-1 and B-1 are 3.05 and 2.5% per °C respectively. In addition, these results support how important the thermal performances are in LIB.

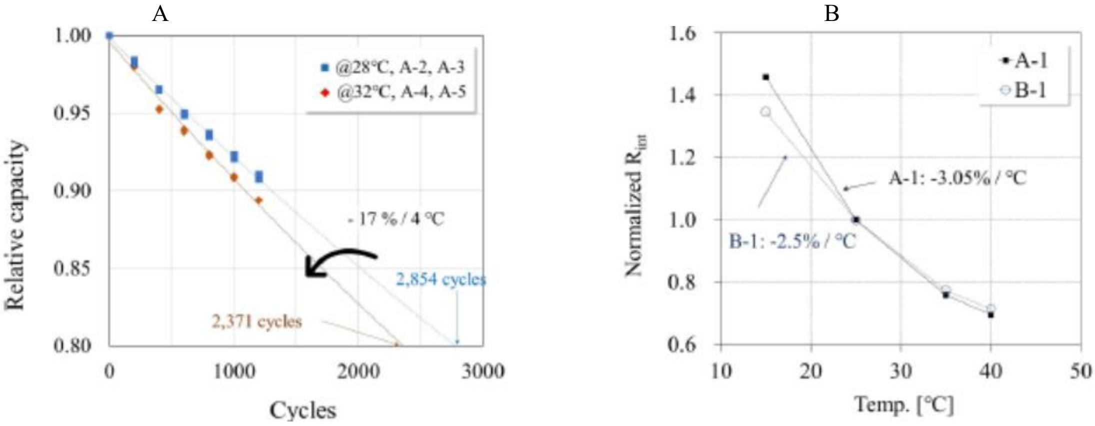

Figure 4**:** Sensitivity test results to the temperature of lifecycle of LiB. **(a)** Lifecycle test results at 28 °C and 32 °C. The number of cycles versus relative capacity. The other test conditions are cycle depth = 97%, and 0.5 C-rate. The degradation trend is fitted to an exponential equation up to the 0.8 relative capacity. **(b)** Normalized capacity rating Vs temperature. of A-1 and B-1 cell is 3.7 and 5.9 mΩ at 25 °C, respectively

Structural Analysis

To find structural causes that determine the performance difference, computed tomography (CT) scanning was carried out on the electrode. With a 0.10 mm spatial resolution of this scanning, the anode and cathode details, such as partial size and dimensions were determined and the tab structure was analyzed. The tab serves to electrically connect the current corrector (CC) attached to the electrode with an external terminal. The tab design factors consider for this research work is; the number, thickness, width, length, and material of tabs, directly affect energy efficiency and heat generation. It was understood from the CT analysis that the tab design affects the performance difference between A-1 and B-1. (See Figure 5 & 6) this can be explained in two parts; firstly, a tab attachment part to a wound cell jelly roll and secondly, tab design from the core cell to external terminal connection inside the case. A structural difference in the connection between the tab and the jelly roll of these two cells has been observed. From A-1 analysis result, it was confirmed that all CCs in a single jelly roll extend from the core cell area and have batch welded to the single tab. This structure is a multi-tab structure in which all the single CC layers are individually tab-connected. On the other hand, the B-3 cell employs the single tab structure in which one cell jelly roll depends on just one tab. Because electrons collected on a single tab have to migrate a long path along with the CC of a jelly roll, it will not only increases the resistance but also induces unwanted energy losses.

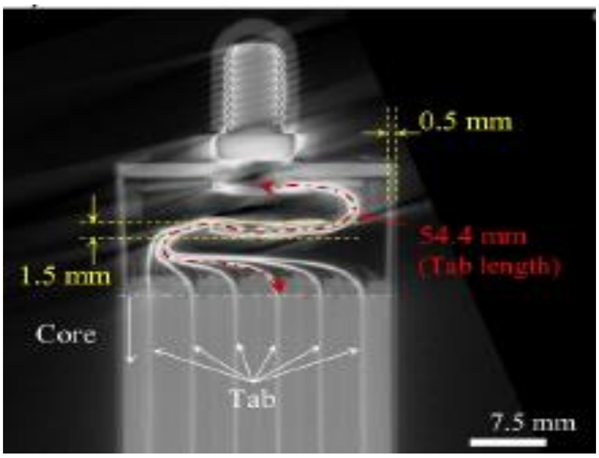

Figure 5: 2D image on cross-section of A-1

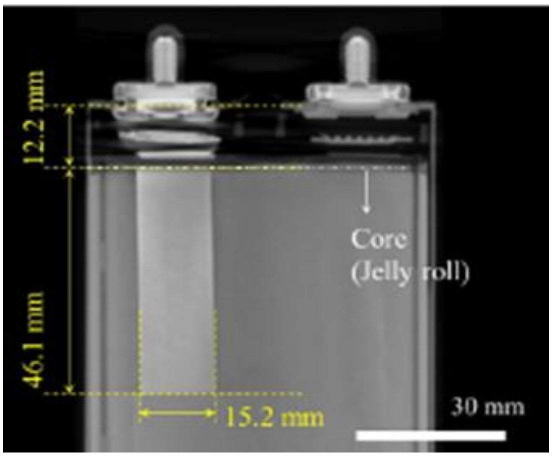

Figure 6: 2D image on xz cross-section of B-1

Figure 5 and 6 shows the single-tab structure of A-1 and the multi-tab structure of B-1 respectively. The tab design difference of both cells from the core cell to external terminal connection and tab resistances were calculated based on the tab geometry analysis. The estimated tab resistance of A-1 and B-2 are shown on Table 1, which is only about 0.07% of the R_{int} measured at SOC = 50% and Temp. = 25°C, whereas the resistance of B-1 is about 3.5%. These calculated results are discussed below.

Table 1: Geometry Analysis From the Cell Core to Terminal of A-1 and B-2 Cells from 3D CT Scanning

Cell	Tab design [mm]			L/(T*W3) [mm^{-1}]	Positive tab Res [μΩ]	Negative tab Res. (Cu) [μΩ]
	Thickness	Width	Length			
A-1	2.5	45.8	14.5	0.063	1.7	1.0
B-1	0.75	15.2	54.4	4.772	126.5	80.2

where L= the length, T = the thickness and W = the width on Table 1. Resistivity (ρ) : ρ_Cu = 1.68 * 108 [Ω·m], ρ_Al = 2.65 * 108 [Ω·m]. - R_{int}): R_{int} of A-1 and B-1 is 3.7 and 5.9 mΩ, respectively. They are measured at SOC = 50%.

Discussion

This study confirmed that the produced Li-on *A*-1 battery has higher energy and power density compared to the SUPPER-B *B*-1 Battery. With the introduction of Li $[Ni_{0.92}Co_{0.06}Al_{0.01}Nb_{0.01}]O_2$ (Nb-NCA93) cathode with a high energy of 869 Wh kg^{-1} the energy density was enhanced. The presence of Nb in the Nb-NCA93 cathode induces the grain refinement of its secondary particle whereby alleviating internal stress and preventing heteroneity of Li-on A-1 concentration during cycling. Therefore, the resulting full-cell reaches full charge within 25-30 minute and retains 85.3% of its initial capacity rating after 1000 cycles (cycle at full depth of discharge). In addition, the Nb-NCA93 cathode generates limited heat under XFC conditions due to refined nanostructure.

On the temperature distribution characteristics between A-1 and B-1 cells both exhibit a temperature increase of 2.93 ^{o}C and 7.33 ^{o}C respectively. It was revealed in the temperature sensitivity evaluation that the lifespan and R_{int} of *A*-1 battery can decrease by 4.25% and by 3.05% respectively when the temperature increases by 1 ^{o}C. As a result, lifespan of *A*-1 battery is 12.5% degraded and R_{int} is 8.9% underestimated, without any compensation to the error.

The investigated results in the CT structural analysis support the electrical and thermal performance difference between two sorts of batteries. It is found that the *A*-1 cells with multiple tabs and a shorter path between the core jelly roll to the terminal has better Front Of Meter (FOM), round-trip electrical efficiency, and thermal performance than the *B*-1 cells having a single tab design and a relatively long path. These tabs act as transferring thermal energy as well as electrical energy. Improvement of the internal tap design of the battery can, hence, be expected to improve the substantial electrical and thermal performance.

The limitations of this paper and future research directions are proposed. First, the FOM proposed here only mathematically explained the correlation with Joule heat but did not verify the absolute amount of heat generated in the actual experiment these are due to different errors like braking error, flux leakage error etc.

However, its heat generate characteristics was confirmed indirectly based on the temperature change result. The surface temperature can be relied on thermal resistance and capacitance characteristics. Surface temperature in operating is affected not only by heat generation, but also by thermal resistance and thermal capacitance. Nevertheless, the theoretical validity of this FOM has been confirmed in various thermal studies (Wang *et al.,* 2017, Un-Hyuck *et al.,* 2022). Furthermore, this FOM can be extended to thermal modeling and thermal characteristics researched.

CONCLUSION

From the results and analysis presented in this paper, we have compared the performance of produced battery A-1 with an LFP battery from a supplier (SUPER-B) B-1 based on multiple perspectives such as the energy density, cycle durability and rate capacity. Thus, to easily evaluate their long duration capability and energy efficiency, a new approach was adopted (FOM) which correlate with key thermal performance indicators. The produced Li-on battery had a better specific power, specific energy, and energy density performance than the SUPER-B, however, their round-trip energy efficiency and heat generation characteristics in terms of operating temperature were relatively the same, especially, in a maximum temperature condition, the temperature change of the A-1 Li-on cell was 29.1 ^{o}C compared to the initial, which was more than twice of the SUPER-B. As a result, more cooling load of Li-on battery was experienced than SUPER-B battery, this enhanced the storage duration longer than SUPER-B. Also, a relatively larger temperature distribution characteristic was confirmed on the Li-on Battery using a high-performance IR camera. Based on the cycling aging and R_{int} characteristics of the *A*-series cells, a 4.25% lifetime reduction and 3.05% underestimated R_{int} values are expected when the measured temperature is measured 1 ^{o}C lower than the actual battery temperature.

Finally, A-1 Lithium-ion batteries offer high energy density and improved thermal performance compared to older battery technologies. This means they can store more energy in a smaller, lighter package, and can operate effectively across a wider temperature range, with few limitations. The results of optimization of the package design of the produced LiB have improved the temperature distribution characteristics. Hence, the efforts proposed in this paper has enhance the capacity rating, energy density, cycle durability, reliability, accuracy, and safety of the of the LiB. By employing the new FOM, temperature distribution analysis, and cell package structure analysis, the balanced performance of batteries was evaluated. We can understand that efficiency, thermal generation, and thermal distribution characteristics are all factors to be considered when designing a Li-on battery for long duration application including optimize tab design for mass production.

ACKNOWLEDGMENT

The authors acknowledge the support of the Nigerian Tertiary Education Trust Fund (TETFund) for providing funding for this research under Institutional Based Research (IBR2023)

REFERENCES

Abakumov, A.M.; Fedotov, S.S.; Antipov, E.V.; Tarascon, J.M. (2020). "Solid State Chemistry for Developing Better Metal Ion Batteries". Nat. Commun, 11, 4976.

Atawi, I.E.; Al-Shetwi, A.Q.; Magableh, A.M.; Albalawi, O.H.(2022). "Recent Advances in Hybrid Energy Storage System Integrated Renewable Power Generation: Configuration, Control, Applications, and Future Directions". Batteries, 9, 29.

BU-302 (2023) "Series and Parallel Battery Configuration". Available online: https://batteryuniversity.com/article/ bu-302-series-and-parallel-battery-configurations

Deng, D. (2015). "Li-Ion Batteries: Basics, Progress, and Challenges". Energy Sci. Eng. 3, 385–418.

Divya, K.C.; Østergaard, J. (**2009). "**Battery Energy Storage Technology for Power Systems—An Overview". Electr. Power Syst. Res, 79, 511–520.

Holechek, J.L.; Geli, H.M.E.; Sawalhah, M.N.; Valdez, R. (**2022**) "A Global Assessment: Can Renewable Energy Replace Fossil Fuels by 2050? Sustainability", 14, 4792

Islam, M.; Omole, A.; Islam, A.; Domijan, A. (2010). "Dynamic Capacity Estimation for a Typical Grid-Tied Event Programmable Li-FePO4 Battery". In Proceedings of the IEEE International Energy Conference and Exhibition (EnergyCon), Manama, Bahrain, 18–22 December 2010; pp. 594–599.

John, B. Goodenough (2011). “Evolution of Strategies for Modern Rechargeable Batteries”. J. Power Sources, 196, 22201.
Liu, C.; Neale, Z.G.; Cao, G. (2016). ”Understanding Electrochemical Potentials of Cathode Materials in Rechargeable Batteries”. Mater. 19, 109–123.

Liu, D.; Cao, G. (2010) “Engineering Nanostructured Electrodes and Fabrication of Film Electrodes for Efficient Lithium Ion Intercalation”. Energy Environ. Sci., 3, 1218–1237.

Nazri, G.-A.; Pistoia, G. (Eds.) (2023). “Lithium Batteries: Science and Technology” Google Books; Springer US: New York City, NY, USA, ISBN 978-0-387-92675-9.

Reddy, M.V.; Subba Rao, G.V.; Chowdari, B.V.R. (2013). ”Metal Oxides and Oxysalts as Anode Materials for Li Ion Batteries”. Chem. Rev. 113, 5364–5457.

Roy, P.; Srivastava, S.K. (2015). “Nanostructured Anode Materials for Lithium Ion Batteries”. J. Mater. Chem. A **2015**, 3, 2454–2484.

Sayed, E. T., Olabi, A. G., Alami, A. H., Radwan, A., Mdallal, A., Rezk, A., & Abdelkareem, M. A. (2023). Renewable energy and energy storage systems. *Energies*, *16*(3), 1415.

Shukla, A.K.; Prem Kumar, T. (2008). “Materials for Next-Generation Lithium Batteries”. Curr. Sci., 94, 314–331.

T. Kowitkulkrai (2019). “ Internal resistance computation of a cylindrical LCO battery for heat generation model”., IOP Conf. Ser. Mater. Sci. Eng. 501 (2019), 012057.

Un-Hyuck Kim, Soo-Been Lee, Nam-Yung Park, Suk Jun Kim, Chong Seung Yoon, and Yang-Kook Sun. (2022). “High-Energy-Density Li-Ion Battery Reaching Full Charge in 12 min.” *ACS Energy Lett.* 7, 3880−3888

Wang, F.; Wu, X.; Li, C.; Zhu, Y.; Fu, L.; Wu, Y.; Liu, X. (2016). “Nanostructured Positive Electrode Materials for Post-Lithium Ion Batteries”. Energy Environ. Sci. **2016**, 9, 3570–3611.

Wang, F.; Harindintwali, J.D.; Yuan, Z.; Wang, M.; Wang, F.; Li, S.; Yin, Z.; Huang, L.; Fu, Y.; Li, L. (2021). “ Technologies and Perspectives for Achieving Carbon Neutrality”. Innovation 2, 100180.

Wu, B.; Ren, Y.; Li, N. (2018) “LiFePO4 Cathode Materials. In Electric Vehicles—The Benefits and Barriers”; Soylu, S., Ed.; IntechOpen: London, UK; Volume 18, pp. 3631–3638; ISBN 978-953-51-6037-3.

Zhang, J.; Zhang, L.; Sun, F.; Wang, Z. (2018). “An Overview on Thermal Safety Issues of Lithium-Ion Batteries for Electric Vehicle Application”. IEEE Access, 6, 23848–23863.

Zu. W, J. MA, L. Zhang, (2017). “Finite element thermal model and simulation for a cylindrical li-Ion battery”. IEEE Access 5 15372–15379.